FORUM GEOGRAFI
ISSN: 0852-0682 | E-ISSN: 2460-3945

HTTPS://JOURNALS.UMS.AC.ID/INDEX.PHP/FG/

Research article

Assessing Spatiotemporal Dynamics of AI-based Land Use and Land Cover through Sentinel-2 Time-Series Imagery: A Case Study of the Shimbay District, Republic of Karakalpakstan, Uzbekistan

Ilyaskhoja Jumaniyazov[1,*], Mukhiddin Juliev[1,2,3], Mamanbek Reimov[1], Rustam Oymatov[1], Aziz Inamov[1], Begench Yunusov[4], Dilbar Abdramanova[5]

[1] Tashkent Institute of Irrigation and Agricultural Mechanization Engineers, National Research University, 100000, Tashkent, Uzbekistan; [2] Tashkent International University of Education, Imam Bukhariy street, Tuzel-2 block, Yashnabad district, Tashkent, Uzbekistan; [3] Tashkent State Technical University, Universitet 2, Tashkent, 100095, Uzbekistan; [4] Ministry of Water Resources of the Republic of Uzbekistan, Karasuv-4, building 11, 100187, Tashkent, Uzbekistan; [5] Karakalpak State University named after Berdakh, 1 Str. Ch.Abdirov, 230112, Nukus, Republic of Karakalpakstan, Uzbekistan.

[*)] Correspondence: ilyasxoja.jumaniyazov@gmail.com

Citation:
Jumaniyazov, I., Juliev, M., Reimov, M., Oymatov, R., Inamov, A., Yunusov, B., & Abdramanova, D. (2026). Assessing Spatiotemporal Dynamics of AI-based Land Use and Land Cover through Sentinel-2 Time-Series Imagery: A Case Study of the Shimbay District, Republic of Karakalpakstan, Uzbekistan. Forum Geografi. 40(1), 44-56.

Article history:
Received: 27 February 2025
Revised: 12 November 2025
Accepted: 17 November 2025
Published: 28 January 2026

Abstract

Land use and land cover (LULC) change is a vital indicator of environmental transformation and sustainable land management, particularly in arid and semi-arid regions such as Karakalpakstan. Although several studies have explored LULC dynamics across Central Asia, most have focused on large-scale or regional assessments, leaving a gap in district-level analyses that capture localized land transformation processes. This study addresses this gap by examining the temporal dynamics of LULC in the Shimbay district, one of the most populous districts in the northern part of the Republic of Karakalpakstan, Uzbekistan. The research aims to identify changes in LULC using Sentinel-2 satellite imagery over 6 years, from 2017 to 2022. The study area was selected based on 10 years of government "Land Fund" data, indicating significant changes in bare land. The satellite images and field measurements were analyzed using ArcGIS 10.4.1. LULC was categorized into five classes: water bodies; vegetation and agricultural land (including flooded mangroves, emergent vegetation, paddy fields, irrigated agricultural lands, cereals, grasses, and non-tree crops); built-up areas; saline land; and bare land. Following classification, 100 random sample points were generated in ArcGIS and verified using Google Earth Pro to ensure classification accuracy. The results showed that the overall accuracy of the LULC classification was 81% (Kappa coefficient = 0.74) in 2017 and 71% (Kappa coefficient = 0.66) in 2022, both within the "substantial" agreement range. The most significant change occurred in vegetation and agricultural lands, with 13,183.38 ha (9.4% of the study area) converted into bare land. These findings provide a detailed understanding of landscape transformation in the Shimbay district and offer policymakers and planners valuable insights to enhance sustainable land management and prevent further land degradation.

Keywords: Land cover; Land use; GIS; Remote sensing; Sentinel-2; Accuracy assessment; Shimbay.

1. Introduction

The implementation of global initiatives to mitigate climate change, promote sustainable development, and safeguard ecosystems and biodiversity is closely linked to United Nations Sustainable Development Goal 13 (Climate action). The term "land cover classification," as defined by the United Nations System of Environmental-Economic Accounting (UN-SEEA), refers to the "physical and biological characteristics of the Earth's surface, encompassing natural vegetation and non-living surfaces (UN, 2019). This is particularly evident in the creation of maps showing changes in land use and cover (LULC) at the global, national, and regional levels (Acar & Zengin, 2023). Land use is the planned application of land management strategies by human agents to utilize land cover. It represents human activities such as industrial zones, residential zones, agricultural fields, grazing, logging, and mining, among others (Teshager & Abeje, 2021; Fatima N and Javed A *et al.,* 2021). In contrast, land cover refers to the characteristics of the earth's surface that are represented in the distribution of vegetation, water, ice, desert, and topography, as well as the immediate subsurface, which includes biota, soil, topography, surface, and groundwater (Nedd *et al.,* 2021).

Furthermore, baseline data on planning, management, and sustainable resource use are derived from our understanding of temporal variations in LULC (Gebeyehu *et al.,* 2019; Paudel *et al.,* 2016; Wulansari, 2017). As a result, to analyze environmental processes and issues and to maintain or improve living standards, land-use data is required. It is particularly crucial to monitor LULC changes frequently in rapidly expanding regions, as unplanned, irregular urban population growth can alter urban climates (Dhakal *et al.,* 2022). Thus, it is critical to understand the patterns and trends in LULC change at the regional, local, and global scales. Preserving the environment while boosting economic and social advantages is the greatest challenge (Islami *et al.,* 2022).

Copyright: © 2026 by the authors. Submitted for possible open access publication under the terms and conditions of the Creative Commons Attribution (CC BY) license (https://creativecommons.org/licenses/by/4.0/).

Land classification research is necessary to manage natural resources and environmental issues and to assess the current state (Aslanov *et al.,* 2023). The natural science community has extensively used satellite images to assess changes in land cover and terrestrial land use at both qualitative and quantitative levels (Salman *et al.,* 2020). Novel insights into the field of large-scale LULC mapping have been made possible by the worldwide consolidation and development of cloud computing platforms, artificial intelligence, machine learning, deep learning, and deep transfer learning; moreover, time series-based techniques and remotely sensed data (Kwan *et al.,* 2020; Sefrin *et al.,* 2020). Seasonal and phenological properties of different LULC classes can be captured by integrating a range of features and spectral-temporal metrics derived from satellite image time series analysis (Htitiou *et al.,* 2021). Classification accuracy will increase when LULC classes are mapped using these characteristics and metrics (Luo *et al.,* 2022).

Geographic information system (GIS) and Remote sensing (RS) communities have long been interested in accurate and current LULC mapping, primarily because it provides important information for understanding human-environment interactions (Nasiri *et al.,* 2022). Compared with traditional surveys, using RS to monitor LULC offers several benefits, including the ability to quickly and accurately create an inventory of broad regions (Deb & Nathr, 2012; Juliev *et al.,* 2019). On a global scale, researchers used GIS and RS to analyze, classify, and assess LULC change dynamics in Sentinel-2 imagery. For example, Islami *et al.* (2022) assessed the accuracy of LULC change analysis using Google Earth in the Sadar Watershed in Indonesia. Zaabar *et al.* (2023) compared Sentinel-2 and Landsat images for LULC classification in an object-based image analysis (OBIA) framework using the Random Forest (RF) and Support Vector Machine (SVM) methods in the Allala watershed of Algeria. The results showed that Sentinel-2 images processed with the RF method achieved higher accuracy than Landsat satellite images. Makar *et al.* (2022) studied the E-Beheira governorate in Egypt using principal component analysis and supervised classification of Sentinel-2 images to enhance LULC classification accuracy. Teshager and Abeje (2021) conducted a LULC change-detection analysis of the Kility Watershed in Ethiopia using Landsat and Sentinel-2 images from 1986 to 2019, employing the maximum likelihood algorithm for supervised classification. Additionally, the accuracy assessment and confusion matrix analysis were conducted to assess the reliability of the LULC analysis. Aimed to evaluate the potential of Sentinel-2 and Landsat-8 images' spectral-temporal metrics by using the Google Earth Engine (GEE) cloud computing to improve the accuracy of the LULC maps, Pande (2022 created a new machine learning algorithm in JavaScript for GEE to classify the LULC map and change detection using Sentinel-2 and Landsat-5 images with a 5-year time difference. The researchers noted that the GEE's ability to perform other analyses on the GEE cloud computing platform is very high.

Remarkable strides have been made in RS technology in recent years to adapt to surface changes on Earth. Sentinel-2 multispectral products from the European Space Agency (ESA) and the European Union (EU) are a major contribution to the Copernicus Program advances, which are used to monitor changes in the Earth's surface (Kumari & Karthikeyan, 2023). Sentinel-2 products are suitable sources for time-series feature extraction because they offer high temporal resolution, short revisit times, and a rich spectral configuration among medium-resolution satellite imagery (Liu *et al.,* 2020). Two Sentinel-2 images (10 m spatial resolution) from 2017 and 2022 were used for LULC mapping and to analyze and detect degraded areas. The region of change between two images of the same scene taken at different times can be detected using change detection. LULC change detection is essential for assessing transitions between land classes. Due to its free and open-access approach, Sentinel-2 data have drawn significant interest from low-income countries, where funding for remotely sensed data acquisition is limited.

Based on the review of existing studies (Gebeyehu *et al.,* 2019; Juliev *et al.,* 2019; Pande *et al.,* 2021; Islami *et al.,* 2022), most LULC analyses have relied on conventional supervised classification approaches, particularly maximum likelihood and object-based methods, applied to relatively small study areas with limited training samples. While these methods are widely used, their reliance on sparse, locally constrained samples often limits classification robustness and generalizability, especially in heterogeneous and degraded landscapes. Limited sample sizes tend to underrepresent spectral variability, leading to uncertainty in accurately delineating complex classes such as degraded bare land. In contrast, recent advances in AI-based classification suggest that large-scale, sample-rich models can substantially improve LULC mapping accuracy by better capturing spatiotemporal dynamics. However, such approaches remain underexplored in arid and semi-arid regions using dense Sentinel-2 time-series data, highlighting a critical methodological gap that this study aims to address.

Therefore, this study focused on a large-scale, sample-based AI land classification model to map the spatial distribution of degraded bare lands using Sentinel-2 imagery. Additionally, the current studies will help monitor changes in land classification over relevant periods. The specific

objectives of this study are i) to map the LULC changes from 2017 to 2022, using Sentinel-2 LULC time series (Living Atlas) data, and ii) to use the statistical analysis to determine the accuracy of the research.

2. Research Methods

2.1. Study Area

Based on the "Land Fund" data of the State Cadastral Chamber of the Cadastral Agency under the State Tax Committee of the Republic of Uzbekistan, used to identify districts (study area) that occupied more bare lands in the agricultural sectors of the Republic of Karakalpakstan (Figure 1). According to the "Land Fund" data, the area of bare land is shown by district in the Republic of Karakalpakstan. So far, the Shimbay district has been a study area with a high tendency toward agricultural graylands.

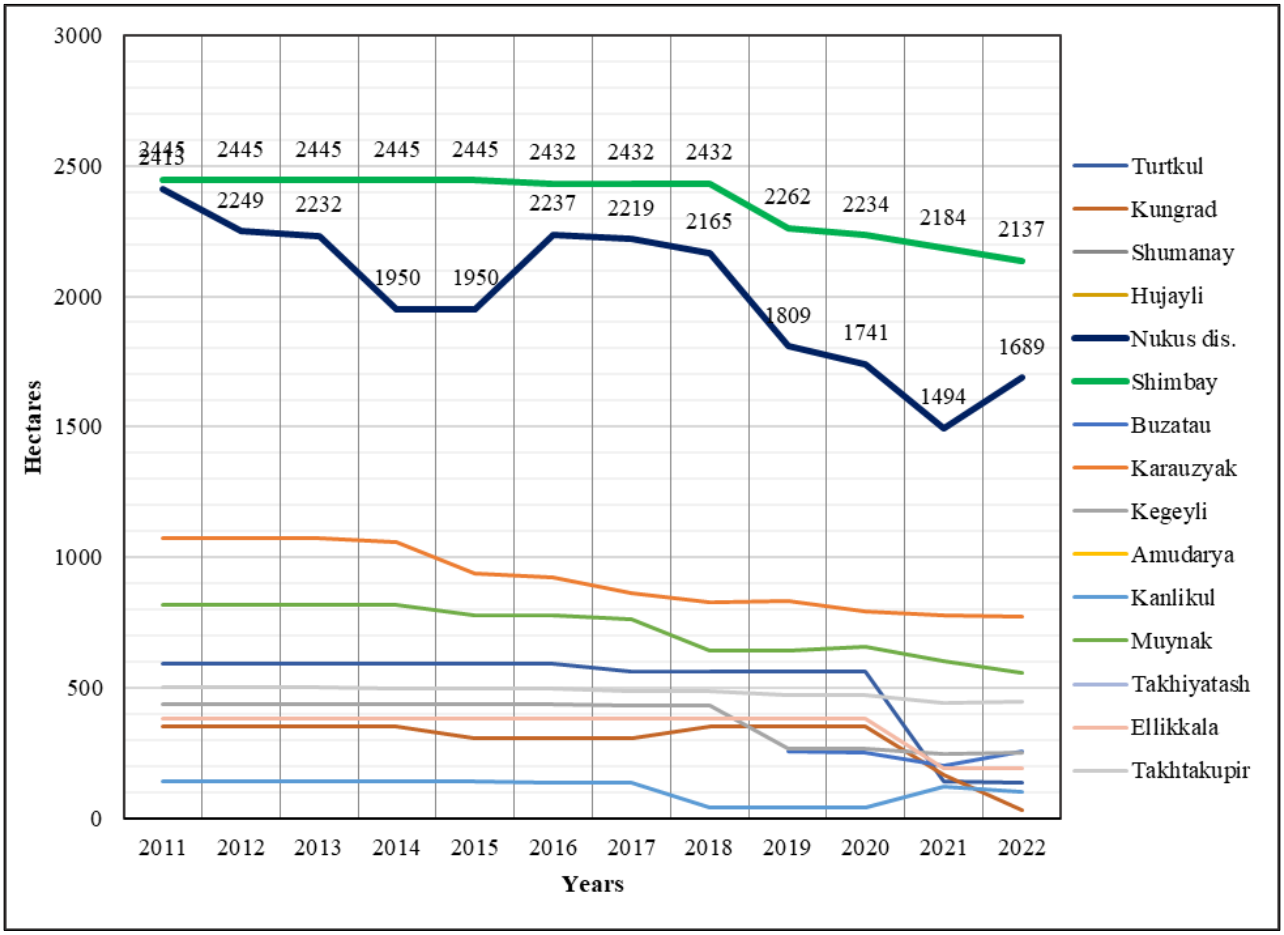

Figure 1. The dynamics of the gray land area in the districts of the Republic of Karakalpakstan. (Source: State Cadastre Chamber of the Cadastral Agency under the State Tax Committee of the Republic of Uzbekistan "Land Fund").

The research selected the Shimbay district of the Republic of Karakalpakstan (Figure 2). The Shimbay district was established in 1927 and borders Bozatau (established in 2019) to the west, Kegeyli to the south, Muynak to the northwest, and the Karauyzak district to the east. Shimbay district is located on the lower right bank of the Lower Amu Darya River (Bekanov *et al.,* 2020). The study area is located between 43°20'20.338"N and 59°58'16.041"E. The district's total area is 1,407 km^2, and the population was 115,061 in 2023 (https://www.citypopulation.de/en/uzbekistan/admin/). The climate is drastically continental. Therefore, summer is hot, winter is cold, and there is slight snow. The annual mean record high temperature is 46.5 °C, and the annual record low temperature is -33.7 °C in winter. Also, the average summer temperature is 26.9 °C, and the average winter temperature is -6.7 °C. The annual mean precipitation is 133 mm, and the annual average number of rainy days is 32 days (www.pogodaiklimat.ru). Vegetation period is 188 days. The Amu Darya River is the only river that runs through the region. Water is used to irrigate crops through large canals in the study area (Rakhmonov *et al.,* 2021). The northern part of the study area is largely bare land, whereas the remainder of the district is used for agriculture, settlement, canals, lakes, and ponds.

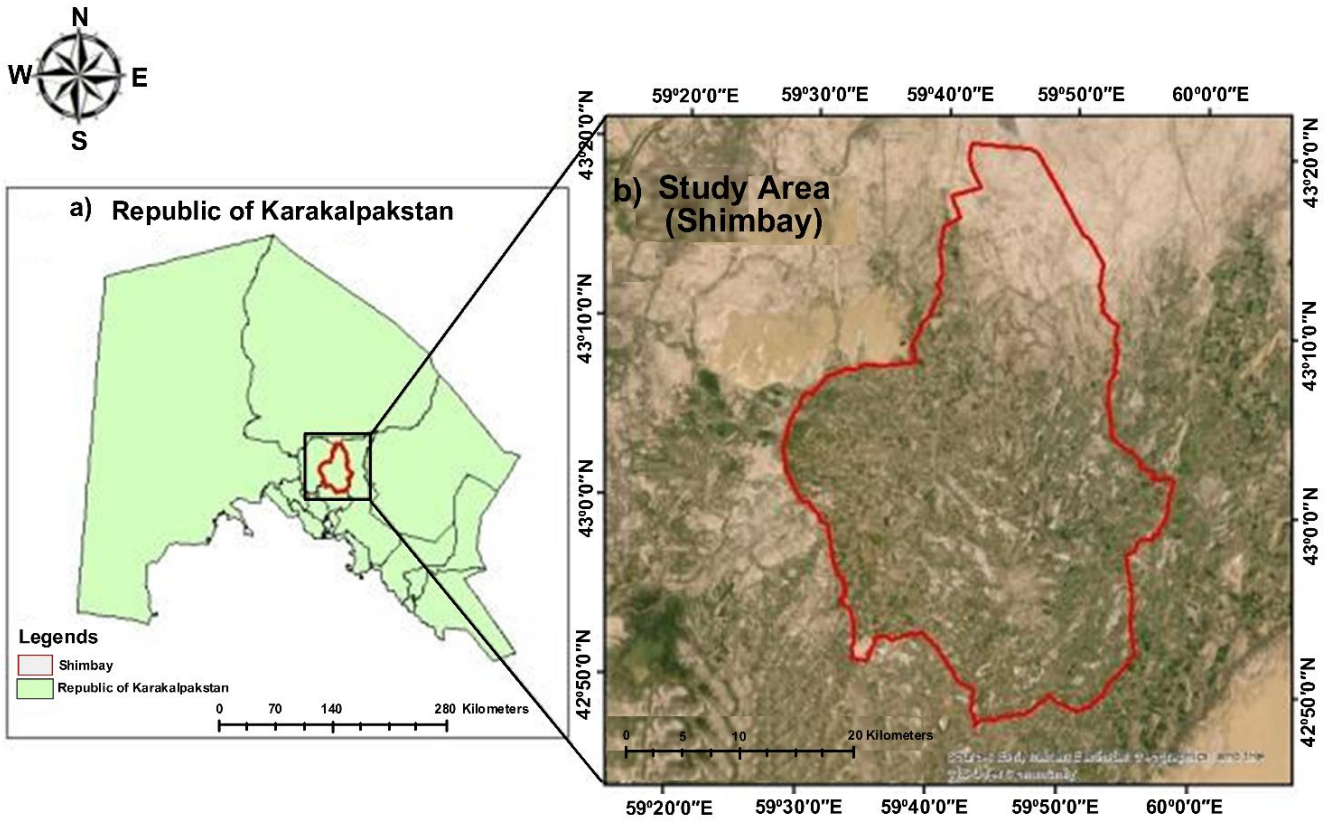

Figure 2. Location of the study area: a) the Republic of Karakalpakstan; b) the satellite image of the Shimbay District.

2.2. Data Collection

Sentinel-2 was developed by the European Space Agency (ESA) and provides high-resolution images of the planet with spectral and temporal resolutions. Thirteen spectral bands are available from the satellite images, with four at 10 meters, six at 20 meters, and three at 60 meters, as shown in Table 1. ESA Sentinel-2 data were used in this study, and two images from 2017 and 2022 were downloaded. Sentinel-2 data were available free of charge at https://www.arcgis.com/home/item.html?id=cfcb 7609de5f478eb7666240902d4d3d. They were available in Tagged Image File Format (TIFF) and projected to the World Geodetic System 1984 (WGS-84) with datum zone 40N.

Table 1. Details Of Satellite Data Acquisition.

Satellite	Sensor	Row/ Path	Date Acquisition	Spectral Bands (nm) (Using bands for layer stack)	Resolution (m)	Data Source
Sentinel-2	Thematic	42/58	01.01.2017 01.01.2022	Band 1 (Coastal): 433-453 Band 2 (Blue): 458-523 Band 3 (Green peak): 543-578 Band 4 (Red): 650-680 Band 5 (Red edge): 698-713 Band 6 (Red edge): 733-748 Band 7 (Red edge): 773-793 Band 8 (NIR): 785-899 Band 8A (NIR narrow): 855-875 Band 9 (Water vapor): 930-950 Band 10 (SWIR Circus): 1365 Band 11 (SWIR): 1565-1655 Band 12 (SWIR): 2100-2280	60 10 10 10 20 20 20 10 20 60 60 20 20	https://www.arcgis.com/apps/mapviewer/index.html?layers=cfcb7609de5f478eb7666240902d4d3d

2.3. Land Cover Classes

Table 2 describes the five land classes that follow: water bodies, Vegetation and Agricultural lands, built-up areas, saline lands, and bare lands, along with the characteristics used in the classification process. In the classification process, we merged vegetation and agricultural land, as shown in the table below.

Table 2. Characteristics Of Each LULC Classification Pattern.

Land use and Land cover types	Descriptions
Waterbody	Rivers, ponds, lakes, and flooded salt plains.
Vegetation and Agricultural Lands	Flooded mangroves, emergent vegetation, rice paddies, and other heavily irrigated and inundated agriculture. / Cereals, grasses, and crops not at tree height; examples: corn, wheat, soy, fallow plots of structured land.
Built-up area	Houses, dense villages/towns/cities, paved roads, and asphalt.
Saline land	The soil contains high concentrations of soluble salts, which often create adverse conditions for plant growth. White or grayish surface crusts, often bright in satellite imagery, are common in these areas due to salt accumulation.
Bare land	Natural meadows and fields with sparse to no tree cover, pastures, and moderate to sparse cover of bushes, shrubs, and tufts of grass.

2.4. Pre-Processing and Image Classification

Sentinel-2's annual images are generated from Impact Observatory's deep-learning AI land classification model using a massive training dataset of billions of human-labeled image pixels. After downloading the Sentinel-2 images to the computer, the data were imported into ArcGIS 10.4.1 to derive the study area data from the Sentinel-2 image tiles. The study area was clipped using the Geoprocessing clip function in the menu bar. Then, the raster-to-polygon tool was used to create an attribute table containing the values from the image grids. Additionally, after creating the attribute tables for the images, the dissolve function was used to combine identical values. The next step is to apply the symbology function to each layer's properties. In this step, we can select the appropriate colors for land types in the study area.

This step involves applying a classification algorithm to assign pixels in a satellite image to predefined land-cover classes based on training data. The classifier uses spectral and index information to assign labels to classes such as forest, urban, water, and agricultural land. In this analysis, supervised classification was used to classify the land classes.

Geometric correction is a preprocessing step in remote sensing that aligns raw image data with a known coordinate system and corrects for sensor errors, Earth curvature, topographic relief, and satellite motion to produce a geometrically accurate image. However, in the Sentinel-2 images, no additional geometric correction is needed because they are already geometrically corrected (orthorectified). In the research, 100 random samples were used for each of the years 2017 and 2022. The accuracy assessment is calculated manually. Nevertheless, the LULC images were downloaded using the Impact Observatory deep learning land-classification model via the Living Atlas platform.

2.5. Accuracy Assessment

For both pre- and post-classified images, accuracy assessment is crucial. A total of 100 randomly selected points were used to validate and assess classification accuracy. To provide a numerical description of the spectral features of each land-cover class, random points are used to identify regions representing each desired land-cover class (Islami *et al.,* 2022). Random points are automatically generated by using the "Create Accuracy Assessment Points" tool of the ArcGIS 10.4.1 software. Based on the confusion matrices, global quality metrics such as Overall Accuracy (OA) and Cohen suggested the Kappa coefficient (K) (Equation (1) and (2)) result be interpreted as follows (Table 3): values ≤ 0 as indicating no agreement and 0.01–0.20 as none to slight, 0.21–0.40 as fair, 0.41– 0.60 as moderate, 0.61–0.80 as substantial, and 0.81–1.00 as almost perfect agreement (McHugh, 2012).

Moreover, the class-level user's accuracy (UA) and producer's accuracy (PA) were calculated (Equations (3) and (4)) to evaluate the impact of Impact Observatory's deep-learning AI land classification model on LULC classification (Nasiri *et al.,* 2022). Equations 1-4 are used in this study to compute the metrics described above. Where TS is the total sample, TS2 is the total sample 2, TCS is the total corrected sample, UA is the user's accuracy, and PA is the producer's accuracy.

$$Overall\ accuracy = \frac{Total\ number\ of\ correctly\ classified\ pixels(Diagonal)}{Total\ number\ of\ reference\ points} * 100 \quad (1)$$

$$Kappa\ Coefficient = \frac{(TS * TCS) - \sum(Column\ Total * Row\ Total)}{TS^2 - \sum(Column\ Total - Row\ Total)} \quad (2)$$

$$UA = \frac{Number\ of\ Correctly\ Classified\ Samples\ in\ each\ Class}{Number\ of\ Samples\ Classified\ to\ that\ Class} \quad (3)$$

$$PA = \frac{Number\ of\ Correctly\ Classified\ Samples\ in\ each\ Class}{Number\ of\ Samples\ from\ Reference\ Data\ in\ each\ Class} \quad (4)$$

Table 3. Standards for evaluating Kappa Coefficient (Islami et al., 2022).

No	Kappa statistics	Strength of agreement
1	<0	Poor
2	0.001 — 0.20	Slight
3	0.21 — 0.40	Fair
4	0.41 — 0.60	Moderate
5	0.61 — 0.80	Substantial
6	0.81 — 1	Almost perfect

The flowchart presented in the diagram (Figure 3) reflects a robust, logical, and data-driven approach to land use and land cover classification using remote sensing and GIS technologies. Each step—from pre-processing to post-classification ensures the accuracy and practical value of the final map. With the increasing availability of satellite imagery and advancements in classification algorithms, such workflows are becoming indispensable in modern geospatial analysis and sustainable land management.

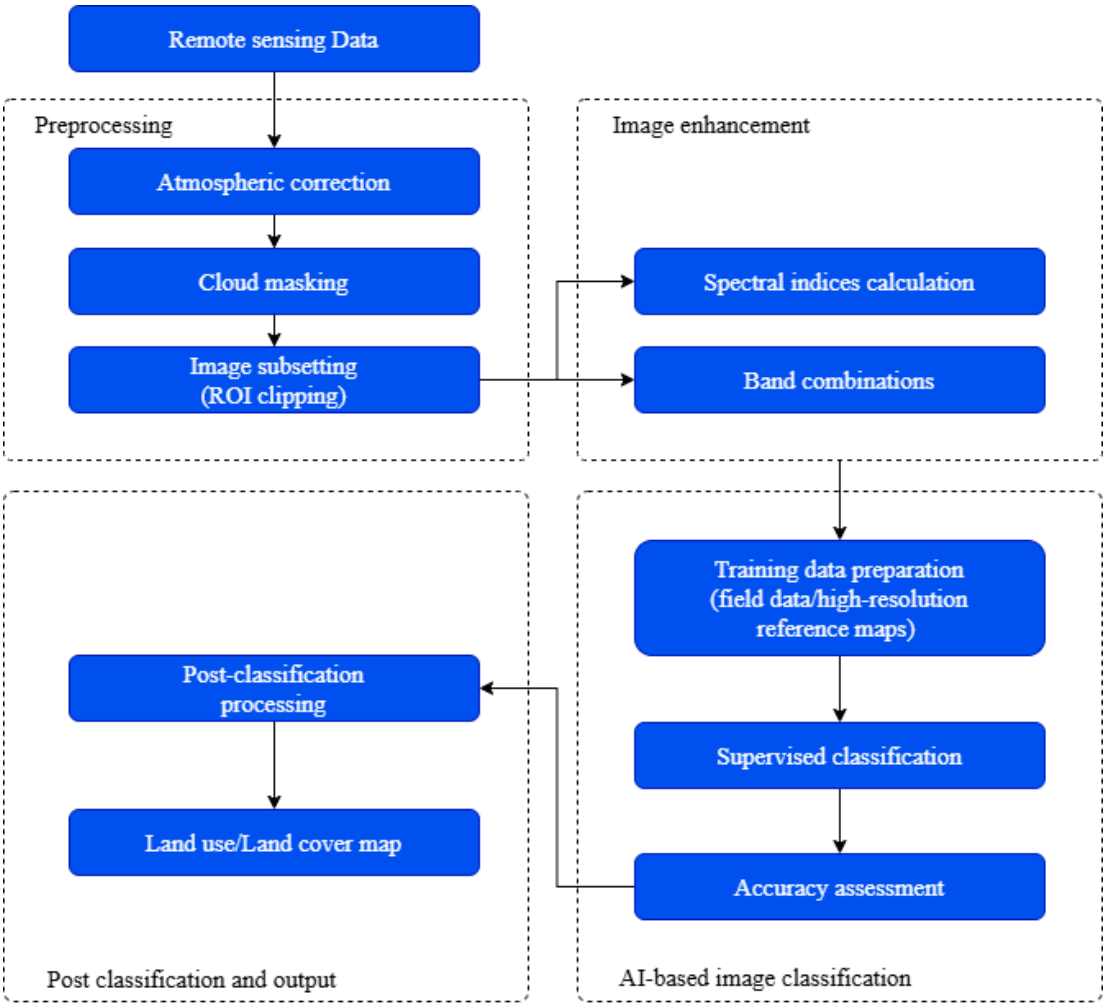

Figure 3. Flowchart of the Proposed Methodology.

3. Results and Discussion

3.1. Accuracy Assessment

To validate the precision of the aforementioned classification data, accuracy assessment is a crucial step in image classification (Foody, 2020). The statistical calculations for the LULC analysis were conducted using 100 randomly selected ground-truth data points to establish overall accuracy and Kappa statistics for the classified images by year, without visiting the study area.

Random points were selected from the classified images and cross-referenced with high-resolution imagery from Google Earth Pro and with ground-truth points for verification.

Accuracy assessment was conducted using the Spatial Analyst tool in ArcGIS 10.4.1. Using the "Create Accuracy Assessment Points" tool, the spatial analyst generated 100 random points in the study area. The generated random points were converted to KML format using the ArcGIS 10.4.1 software Conversion tool. The converted KML file was imported into Google Earth Pro, and the sampled random points class in both ArcGIS and Google Earth Pro were compared to identify the interconnection between them. If the classified value matches the ground truth, the input value will be kept; if it does not, it will be changed to the appropriate class value and after the assessment, used the "Compute Confusion Matrix" tool to automatically calculate the Overall Accuracy, Producer Accuracy, User Accuracy, and Kappa statistics in ArcGIS 10.4.1 and Excel (Skidmore, 1999).

The output of this tool will be used to calculate the Overall Accuracy and Kappa Coefficient using the formulas for Overall Accuracy given above (Equations (1) and (2)). User's accuracy (Equation (3) refers to the commission error, which arises when a pixel is incorrectly assigned to a specific class. It can be computed by dividing the number of accurately classified pixels belonging to a particular class by the total number of pixels assigned to that class. Producer's accuracy (Equation (4), also referred to as the omission error) occurs when a pixel that should belong to a specific class is not included in that class. It is calculated by dividing the number of accurately classified pixels by the total number of reference pixels for that particular class (Congalton, 1991). The accuracy outcomes for classified images from both years are presented in Table 4.

Table 4. Accuracy Assessment Result Of LULC Images.

Land use cover	Sentinel-2 2017		Sentinel-2 2022	
	UA	PA	UA	PA
Waterbody	-	-	-	-
Vegetation and Agricultural Lands	89.8	80.3	83.7	69.5
Built-up area	100	100	57.1	80
Saline land	100	50	100	50
Bare land	64.9	82.7	58.1	73.5
Overall Accuracy		81		71
Kappa Coefficient		0.74		0.66

In the water body, the land-cover class does not have overlaid random points in both years. Therefore, Table 4 does not give data for UA and PA. The mean overall accuracy is 76%, and the mean overall Kappa Coefficient is 0.7%. According to the Kappa Coefficient (Table 4), both 2017 and 2022 images belong to the "Substantial" category.

3.2. LULC Pattern of Shimbay in 2017 and 2022

The acquired Sentinel-2 images were classified using the Observatory's deep-learning AI land classification model. The classified image analyses are given in Figure 4. The research period is from 2017 to 2022. The total area of the study region was 139971.7 ha. The total area classification value is provided in Table 5. According to the 2017 analysis, vegetation and agricultural land were the largest land-use classes, accounting for 72,024.2 ha (51.43% of the total area), and bare land was the second-largest, accounting for 54,032.1 ha (38.6%). The remaining land-use cover types were built-up areas (9,136.9 ha; 6.5%), saline land (4,362.27 ha; 3.1%), and water bodies (416.23 ha; 0.3%) of the total area of the study area. In the 2022-year analysis, vegetation and agricultural lands covered 68,022.9 ha (48.6%), and bare land occupied 62,032.2 ha (44.3%), ranking first and second, respectively, as in the 2017 year. According to the other land use classes, built-up area, saline land, and water body classes occupied 9015.94 ha (6.4%), 770.21 ha (0.6%), and 130.97 ha (0.09%), respectively.

Table 5. Results of the LULC Classification of Images Showing the Area of Each Category and Category Percentages for the Shimbay District.

Land cover classes	2017		2022	
	Area, ha	Area, %	Area, ha	Area, %
Water body	416.23	0.30	130.97	0.09
Vegetation and Agricultural Lands	72,024.20	51.43	68,022.90	48.6
Built-up area	9,136.90	6.53	9,015.94	6.44
Saline land	4,362.27	3.12	770,21	0.55
Bare land	54,032.10	38.60	62,032.20	44.32
Total area	139,971.70	100	139,972.22	100

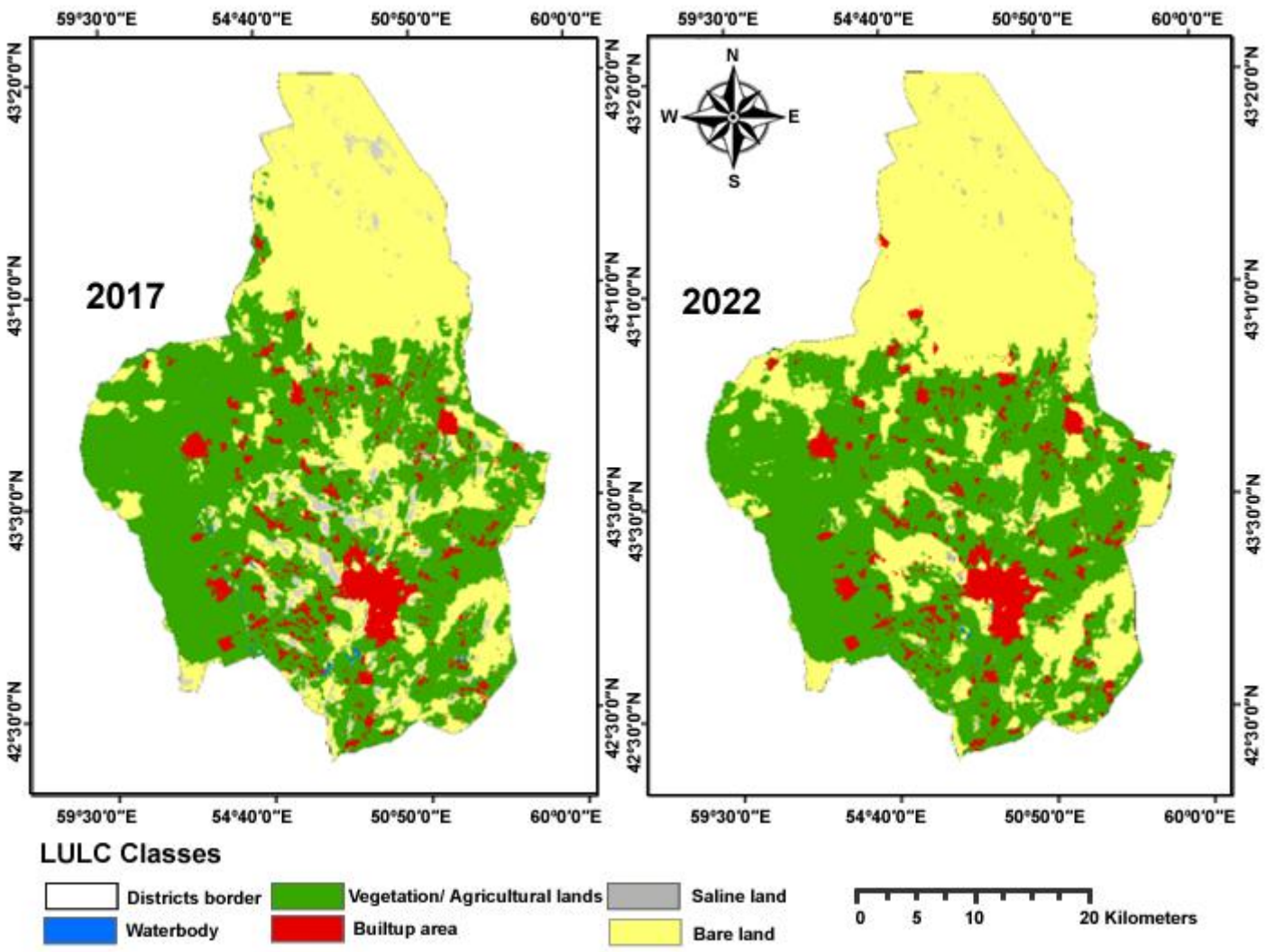

Figure 4. LULC classified Maps of the Study Area from 2017 to 2022.

3.3. LULC Change Detection from 2017 to 2022

Figure 5 shows the changes in land cover classes between 2017 and 2022. The profound changes occurred in vegetation, agricultural, and saline lands, totaling -4,001.3 ha and -3,592.06 ha, or -5.5% and -82.3% of the area of the use category. In addition, the smallest decreases were recorded in the water body and built-up areas, at -285.26 ha (68.5%) and -120.96 ha (1.3%) of the total area, respectively. Just a bare land cover class occurred, increasing by 14.8% during the research period, totaling 8000.1 ha in the use category.

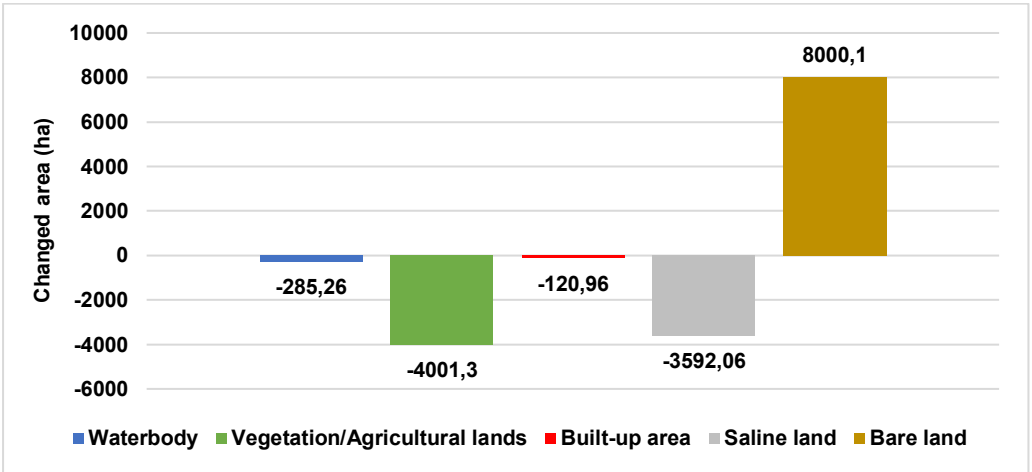

Figure 5. Areal Changes in the Study Area between 2017 and 2022.

3.3. LULC Transitions

This part examined changes in land use and land cover using LULC image analysis of 2017 and 2022 to identify class changes between the initial and final years (Figure 6). The noticeable changes occurred between Vegetation and Agricultural lands and Bare lands: 131,83.38 ha of Vegetation and Agricultural lands changed into Bare lands, which is 9.4% of the study area. However, the next change is the reverse of the previous change: bare land was converted to vegetation and agricultural land, totaling 7604.95 ha, representing 5.4% of the study area. The remaining land-cover changes differed between the same and other land-cover types, as shown in Figure 7.

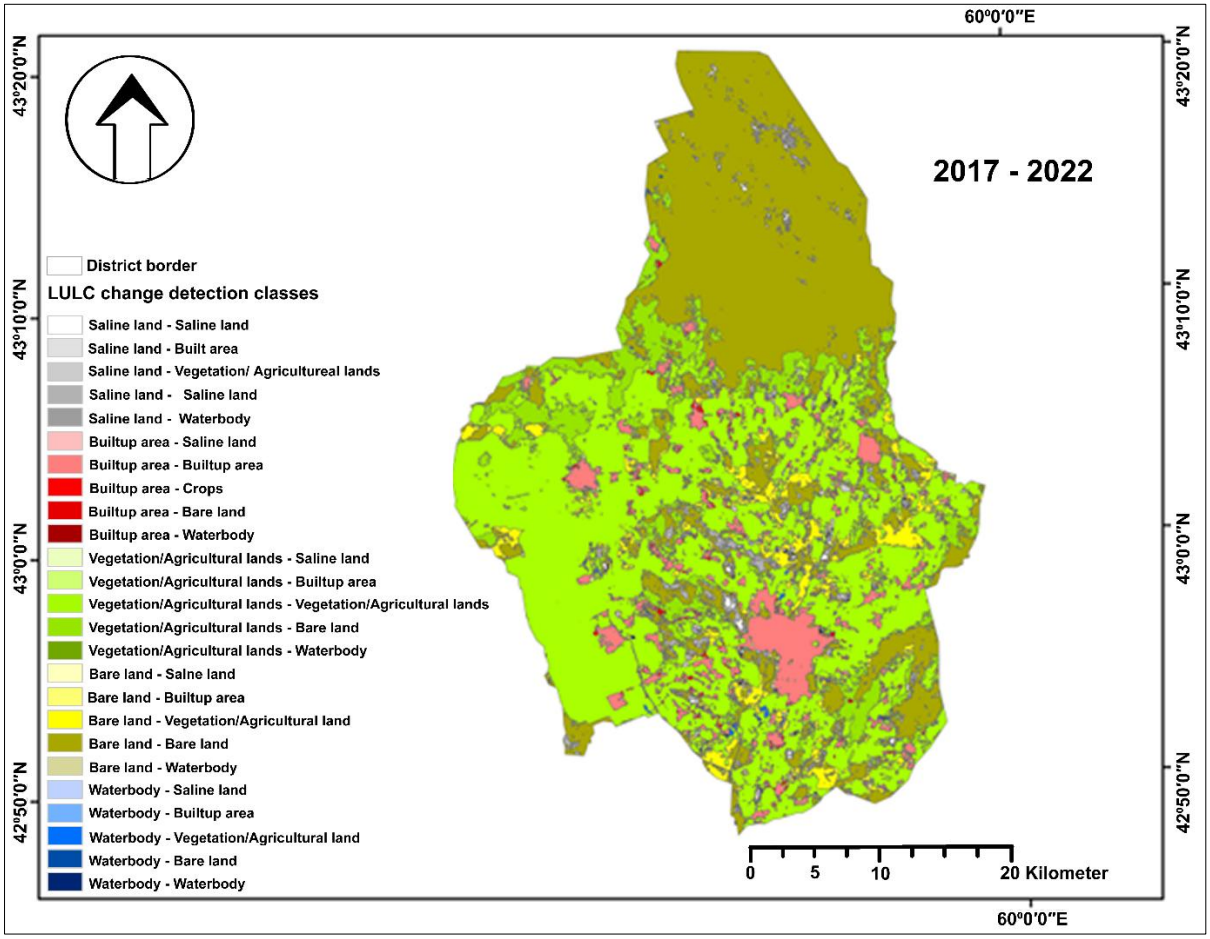

Figure 6. LULC Change Detection Map for 2017-2022.

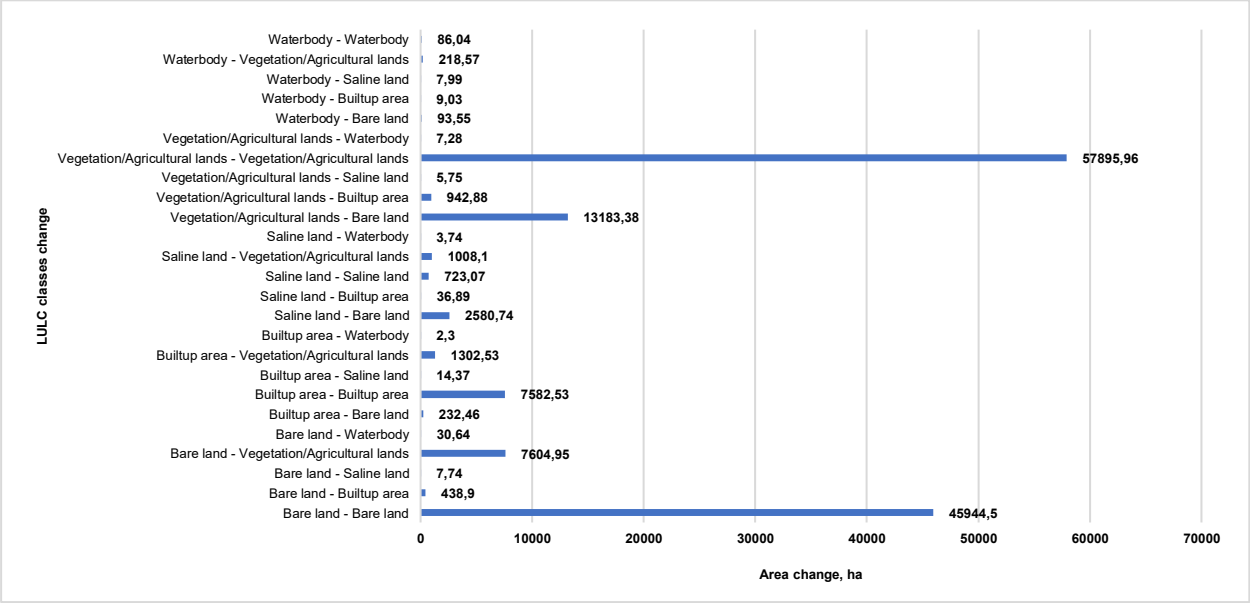

Figure 7. LULC Change Detection Between 2017 and 2022.

3.4. Transition Matrix

The land-cover transition matrices in Table 6 provide detailed information on transformations among land-cover classes during 2017-2022. Analyzing the land cover change between 2017 and 2022 (Table 6), it is clear that the saline lands recorded (experienced) the most significant transformation, with a total of 3,629.5 ha being converted to various land cover types, including built-up area, vegetation and agricultural lands, bare land, and water bodies. Additionally, the water body land cover class is among the most significantly transformed, with a 79.3% change to other land cover classes.

During the same period, the remaining land-cover classes changed by less than 20%, including 13,183.4 ha of vegetation and agricultural land, mostly converted to bare land, and 942.9 ha to built-up areas. Moreover, the built-up and bare land transformations partially altered vegetation and agricultural land by 1,302.5 ha and 7,605 ha, respectively.

Table 6. Transition Matrix of Land Cover Changes (ha), 2017-2022 Years.

Land cover classes		2022 Saline land	Built-up area	Vegetation and Agricultural lands	Bare land	Water body	Total
2017	Saline land	723.07	36.89	1,008.10	2,580.74	3.74	4,352.54
	Built-up area	14.37	7,582.53	1,302.53	232.46	2.3	9,134.19
	Vegetation and Agricultural lands	5.75	942.88	57,895.96	13,183.38	7.28	72,035.25
	Bare land	7.74	438.9	7,604.95	45,952.24	30.64	54,034.47
	Waterbody	7.99	9.03	218.57	93.55	86.04	415.18
	Total	758.92	9,010.23	68,030.11	62,034.65	130	139,971.63

4. Discussion

Using AI-based classification algorithms for Sentinel-2 imagery, the study provides a thorough evaluation of land-use and land-cover (LULC) changes across the Shimbay district from 2017 to 2022. Sentinel-2 high-resolution 10x10 m (Delwart, 2015) LULC maps and quantitative summaries for all major land cover types, including built-up areas not previously mapped in the literature, were produced district-wide. The overall accuracy of the AI-based classification method exceeded 85% (Karra et al., 2021), demonstrating the efficacy of automated classification models in generating dependable and geographically consistent LULC datasets. When applying high-resolution LULC products to region-specific studies, careful map selection and local validation are crucial. Xu *et al.* (2024) conducted a thorough comparative validation of the 10 most recent 10 m global land cover maps, revealing significant variability in class-wise accuracy and regional performance. Li *et al.* (2024) demonstrated enhanced generalization and robustness across multiple datasets by introducing a novel learning paradigm for foundation-model-based remote sensing change detection. This highlights the growing potential of large-scale AI models to capture intricate spatiotemporal land-surface dynamics relevant to this study. Also, Aziz *et al.* (2024) showed that machine learning-based classification of remote sensing data can efficiently map forest cover with high accuracy. This supports the applicability of the AI-based methods used in this study and highlights the suitability of data-driven approaches for detailed land-cover characterization. Using remote sensing data, Zafar *et al.* (2024) assessed the effectiveness of several machine learning algorithms for LULC mapping. They found that algorithm selection significantly affects classification accuracy, underscoring the need for careful model selection and validation in AI-based LULC mapping studies such as the current work. Another researcher, Peng *et al.* (2024), conducted a comparative analysis of pre-trained CNN-based deep learning models for crop monitoring using remote-sensing LULC and land-change data. Also, He *et al.* (2024) demonstrated the efficacy of a deep learning-based temporal semantic segmentation framework for time-series land cover change detection in capturing intricate spatiotemporal dynamics. Another study, Tejasree and Agilandeeswari (2024), highlighted the benefits of sequence-based deep learning models for capturing intricate land-surface patterns pertinent to time-series remote sensing analyses, demonstrating that deep LSTM networks efficiently model temporal and spectral dependencies for LULC classification of hyperspectral imagery.

The current study offers numerous methodological improvements over the work of Bekanov et al. (2020), who used Landsat-8 images (30×30 m) (Vaughn Ihlen, 2019) and a traditional unsupervised pixel-based methodology to map only agricultural areas within the Shimbay region. First, Sentinel-2 imagery enabled more accurate land-cover classification owing to its enhanced spectral sensitivity and finer spatial resolution. Second, the current study identified patterns of land alteration and degradation that are not apparent in single-year evaluations, using a multi-temporal analysis covering 2017–2022. This temporal depth provides important information on

ongoing changes in vegetation decline, agricultural land expansion, and potential early indicators of desertification. Third, the use of AI-based categorization eliminated the need for manual photo downloads and GIS-based reclassification, which are typical of conventional approaches, by automating the production of training data. This invention increased accuracy and reproducibility while reducing analytical time. However, some restrictions still exist. Seasonal land-use differences may be missed when using annual composite images. For example, croplands harvested in early summer may show as bare soil for the rest of the year. The paucity of pre-2017 imagery in the Sentinel-2 archive also prevented the analysis from extending back to earlier decades, limiting the long-term historical perspective on LULC change.

The results of this study are consistent with those of Bekanov, who also demonstrated the usefulness of GIS and remote sensing for LULC mapping in the Shimbay district. By leveraging AI-based time-series analysis and achieving greater geographical precision, the current study builds on their contribution. Moreover, the integration of artificial intelligence techniques into land cover classification reflects an emerging consensus in recent research. According to studies like those by Maxwell *et al.* (2018) and Pelletier *et al.* (2019)Machine learning and deep learning algorithms improve classification accuracy, automate analysis, and reduce reliance on manually collected field data. In dry and semi-arid regions such as the Aral Sea region, where regular monitoring is essential for understanding environmental degradation and informing policy responses, these methods are particularly useful.

The results highlight the potential of AI-enhanced Sentinel-2 time-series analysis for accurate detection of land-cover changes, despite certain data constraints. Regional planning and sustainable land management can be substantially aided by the Impact Observatory Global LULC dataset when combined with high-resolution imagery. These findings highlight the need for governments to focus on protecting agricultural land and mitigating degradation. Seasonal composites and predictive models should be used in future studies to estimate potential LULC changes in the larger Aral Sea basin.

5. Conclusion

The research was conducted in the western part of Uzbekistan, in the Republic of Karakalpakstan, which is surrounded by the Kyzylkum Desert and the Ustyurt Plateau. This research used the Impact Observatory's deep-learning AI-based classification model on Sentinel-2 data. During the research, some positive and negative outcomes of the Impact Observatory's deep-learning AI land classification model were identified. The advantage of this model is that it helps clarify land types in the research area that were previously unfamiliar and facilitates analysis of the dynamics of land-type change over the years. Additionally, it requires less time for analysis and mapping than other types of the LULC classification process. Because Sentinel-2 10m Land Use and Land Cover Time Series data is included ready classified land classes data on images. On the ArcGIS.com website, information on the LULC classification model accuracy is 85%. In our research work, the average overall accuracy was 76% in two 2017-2022 years. The Kappa statistics results of the classified images belonged to the "Substantial" class. Moreover, user accuracy and producer accuracy also help to improve the precision of the classified LULC images of the Impact Observatory's deep-learning AI model.

These findings are vital for policymakers and environmental managers, providing a basis for creating informed conservation strategies. The study highlights the importance of sustainable development practices to reduce negative effects on these important natural resources. The AI models utilized in this research can act as a blueprint for similar studies in other areas, improving our ability to manage and safeguard natural landscapes in the face of increasing environmental challenges. In conclusion, the result showed that the Sentinel-2 Land Use and Land Cover Time Series data can be usable for mapping and analyzing LULC changes. In addition, the Overall Accuracy and Kappa Coefficients results also showed the acceptability of the classified images. We suggest that in the case of the Republic of Uzbekistan and Karakalpakstan, need to improve the quantity and quality of the LULC classification research works to understand the change of the land cover by the impact of global climate change and the impact of the Aral Sea dust storms.

Acknowledgements

This research was conducted at the "Joint Research Center for Geoinformatics" at the National Research University "Tashkent Institute of Irrigation and Agricultural Mechanization Engineers." Also, thanks to the ArcGIS company developers for providing us with ready satellite image data to conduct research on Land Use and Land Cover Classification.

Author Contributions

Conceptualization: Jumaniyazov, I.; **methodology**: Jumaniyazov, I.; **investigation**: Jumaniyazov, I., Juliev, M., Reimov, M., Oymatov, R.,; **writing—original draft preparation**: Jumaniyazov, I.,; **writing—review and editing**: Jumaniyazov, I.,; **visualization**: Jumaniyazov, I.,. All authors have read and agreed to the published version of the manuscript.

Conflict of interest

The author declares that he has no known competing financial interests or personal relationships that could have appeared to influence the work reported in this paper.

Data availability

Data is available upon Request.

Funding

This research received no external funding.

References

Acar, R.U., ZengiN, E. (2023). Performance assessment of Landsat 8 and Sentinel-2 satellite images for the production of time series land use/land cover (LULC) maps. *J. Sci.* Rep.-Rep. -A, 1–15. doi: 10.59313/jsr-a.1213548

Aslanov, I., Jumaniyazov, I., Embergenov, N., Allanazarov, K., Khodjaeva, G., Joldasov, A., Alimova, S. (2023). Remote Sensing for Land Use Monitoring in the Suburban Areas of Tashkent, Uzbekistan, XV International Scientific Conference "INTERAGROMASH 2022, Lecture Notes in Networks and Systems. *Springer International Publishing, Cham, 1899*–1907. doi: 10.1007/978-3-031-21219-2_211

Aziz, G., Minallah, N., Saeed, A., Frnda, J., Khan, W., (2024). Remote sensing basedsensing-based forest cover classification using machine learning. *Sci. Rep.* 14, 69. doi: 10.1038/s41598-023-50863-1

Bekanov, K., Safarov, E., Prenov, S., Uvraimov, S., & Yusupov, B. (2020). Creating land use/land cover map using methods gis and remote sensing (on the example the chimbay district of the karakalpakstan republic). International *Journal of Pharmaceutical Research,* 12(3), 1704-1708. doi: 10.31838/ijpr/2020.12.03.231

Bekanov, K., Safarov, E., Prenov, Sh., Uvraimov, S., Yusupov, B. (2020). Creating land use / land cover map using methods gis and remote sensing (on the example the chimbay district of the karakalpakstan republic). Int. J. Pharm. Res. 9(3), 12. doi: 10.31838/ijpr/2020.12.03.231

Blanka, V., Par Johan, A., (2015). *New sensors benchmark report on Sentinel-2A. Commission of the European Union. Joint Research Centre. Institute for the Protection and the Security of the Citizen..Citizen.* Publications Office, LU.

City Population. (2025). *Uzbekistan: Administrative Division.* Retrieved from https://www.citypopulation.de/en/uzbekistan/admin/

Congalton, R.G. (1991). A review of assessing the accuracy of classifications of remotely sensed data. *Remote Sens. Environ, 37*, 35–46. doi: 10.1016/0034-4257(91)90048-B

Deb, D.S.K., Nathr, R.K. (2012). *Land use/cover classification- An introduction review and comparison.* Retrieved from https://globaljournals.org/GJRE_Volume12/2-Land-usecover-classification-An-introduction-review.pdf

Delwart, S. (2015). ESA Standard Document.

Dhakal, S., Kandel, S., Puri, L., Shrestha, S. (2022). Assessment on Land Use Land Cover Mapping:Mapping : Sentinel-2 Versus Landsat-9. *For. J. Inst. For. Nepal,* 19, 56–63. doi: 10.3126/forestry.v19i01.55704

Esri. (2025). *Sentinel-2 10m Land Use/Land Cover Time Series [ArcGIS Online dataset*]. Retrieved from https://www.arcgis.com/home/item.html?id=cfcb7609de5f478eb7666240902d4d3d

Fatima, N., Javed, A. (2021). Assessment of Land Use Land Cover Change Detection Using Geospatial Techniques in Southeast Rajasthan. *Journal of Geoscience and Environment Protection,* 09(12), 299–319. doi : 10.4236/gep.2021.912018

Foody, G.M. (2020). Explaining the unsuitability of the kappa coefficient in the assessment and comparison of the accuracy of thematic maps obtained by image classification. *Remote Sens. Environ,* 239, 111630. doi: 10.1016/j.rse.2019.111630

Gebeyehu, A.E., Chunju, Z., Yihong, Z. (2019). Assessment and Mapping of Land Use Change by Remote Sensing and GIS:GIS : A Case Study of Abaya Chamo Sub-basin, Ethiopia. Nat. Environ. *Pollut. Technol.,* 18.

He, H., Yan, J., Liang, D., Sun, Z., Li, J., Wang, L., (2024). Time-series land cover change detection using deep learning-based temporal semantic segmentation. *Remote Sens. Environ,* 305, 114101. doi: 10.1016/j.rse.2024.114101

Htitiou, A., Boudhar, A., Chehbouni, A., Benabdelouahab, T. (2021). National-Scale Cropland Mapping Based on Phenological Metrics, Environmental Covariates, and Machine Learning on Google Earth Engine. *Remote Sensing,* 13(21), 4378. doi: 10.3390/rs13214378

Islami, F.A., Tarigan, S.D., Wahjunie, E.D., Dasanto, B.D. (2022). Accuracy Assessment of Land Use Change Analysis Using Google Earth in Sadar Watershed Mojokerto Regency. *IOP Conf. Ser. Earth Environ. Sci.,* 950, 012091. doi: 10.1088/1755-1315/950/1/012091

Juliev, M., Pulatov, A., Fuchs, S., Hübl, J., (2019). Analysis of Land Use Land Cover Change Detection of Bostanlik District, Uzbekistan. *Pol. J. Environ. Stud.,* 28, 3235–3242. doi: 10.15244/pjoes/94216

Karra, K., Kontgis, C., Statman-Weil, Z., Mazzariello, J. C., Mathis, M., & Brumby, S. P. (2021). Global land use/land cover with Sentinel 2 and deep learning. In 2021 IEEE international geoscience and remote sensing symposium IGARSS. *IEEE,* 4704-4707.

Kumari, A., Karthikeyan, S. (2023). Sentinel-2 Data for Land Use/Land Cover Mapping:Mapping : A Meta-analysis and Review. *SN Comput. Sci.,* 4, 815. doi: 10.1007/s42979-023-02214-0

Kwan, C., Ayhan, B., Budavari, B., Lu, Y., Perez, D., Li, J., Bernabe, S., Plaza, A. (2020). Deep Learning for Land Cover Classification Using Only a Few Bands. *Remote Sensing,* 12, 2000. doi: 10.3390/rs12122000

Li, K., Cao, X., Meng, D., 2024. A New Learning Paradigm for Foundation Model-Based Remote-Sensing Change Detection. IEEE Trans. Geosci. *Remote Sensing,* 62, 1–12. doi: 10.1109/TGRS.2024.3365825

Liu, L., Xiao, X., Qin, Y., Wang, J., Xu, X., Hu, Y., Qiao, Z. (2020). Mapping cropping intensity in China using time series Landsat and Sentinel-2 images and Google Earth Engine. Remote Sens. *Environ.,* 239, 111624. doi: 10.1016/j.rse.2019.111624

Luo, C., Zhang, X., Wang, Y., Men, Z., Liu, H. (2022). Regional soil organic matter mapping models based on the optimal time window, feature selection algorithm and Google Earth Engine. *Soil Tillage Res.,* 219, 105325. doi: 10.1016/j.still.2022.105325

Makar R. S., Shahin Sahar A., El-Nazer Mostafa., Wheida Ali. (2022). Development of a PCA-based land use/land cover classification utilizing Sentinel-2time series. *Middle East Journal of Agriculture Research,* 11(2), 630-637. doi: 10.36632/mejar/2022.11.2.42

Maxwell, A.E., Warner, T.A., Fang, F., (2018). Implementation of machine-learning classification in remote sensing: an applied review. *Int. J. Remote Sens.,* 39, 2784–2817. doi: 10.1080/01431161.2018.1433343

McHugh, M.L. (2012). Interrater reliability: the kappa statistic. Biochem. *Medica,* 276–282. doi: 10.11613/BM.2012.031

Nasiri, V., Deljouei, A., Moradi, F., Sadeghi, S.M.M., Borz, S.A. (2022). Land Use and Land Cover Mapping Using Sentinel-2, Landsat-8 Satellite Images, and Google Earth Engine:Engine : A Comparison of Two Composition Methods. *Remote Sens.,* 14, 1977. doi: 10.3390/rs14091977

Nedd, R., Light, K., Owens, M., James, N., Johnson, E., Anandhi, A., (2021). A Synthesis of Land Use/Land Cover Studies: Definitions, Classification Systems, Meta-Studies, Challenges and Knowledge Gaps on a Global Landscape. *Land,* 10, 994. doi: 10.3390/land10090994

Pande, C.B., Moharir, K.N., Khadri, S.F.R., (2021). Assessment of land-use and land-cover changes in Pangari watershed area (MS), India, based on the remote sensing and GIS techniques. Appl. *Water Sci.,* 11, 96. doi: 10.1007/s13201-021-01425-1

Pande, Dr.C. (2022). Land Use/Land Cover and Change Detection mapping in Rahuri watershed area (MS), India using the Google Earth Engine and Machine Learning Approach. *Geocarto International,* 37(26). doi: 10.1080/10106049.2022.2086622

Paudel, B., Zhang, Y., Li, S., Liu, L., Wu, X., Khanal, N.R. (2016). Review of studies on land use and land cover change in Nepal. *J. Mt. Sci.,* 13, 643–660. doi: 10.1007/s11629-015-3604-9

Pelletier, C., Webb, G., Petitjean, F., (2019). Temporal Convolutional Neural Network for the Classification of Satellite Image Time Series. *Remote Sensing,* 11, 523. doi: 10.3390/rs11050523

Peng, M., Liu, Y., Khan, A., Ahmed, B., Sarker, S.K., Ghadi, Y.Y., Bhatti, U.A., Al-Razgan, M., Ali, Y.A., (2024). Crop monitoring using remote sensing land use and land change data: Comparative analysis of deep learning methods using pre-trained CNN models. *Big Data Res.* 36, 100448. https://doi.org/10.1016/j.bdr.2024.100448

Pogoda i Klimat. (2025). *Weather and climate data.* Retrieved from http://www.pogodaiklimat.ru/

Rakhmonov, S., Umurzakov, U., Rakhmonov, K., Bozarov, I., Karamatov, O., (2021). Land Use and Land Cover Change in Khorezm, *Uzbekistan. E3S Web Conf.,* 227, 01002. doi: 10.1051/e3sconf/202122701002

Salman, Md.A., Nomaan, Md.S.S., Sayed, S., Saha, A., Rafiq, M.R., (2020). Land use and land cover change detection by using remote sensing and GIS technology in Barishal district, Bangladesh. *Earth Sci. Malays,* 5, 33–40. doi: 10.26480/esmy.01.2021.33.40

Sefrin, O., Riese, F.M., Keller, S., (2020). Deep Learning for Land Cover Change Detection. *Remote Sens,* 13, 78. doi: 10.3390/rs13010078

Skidmore, A.K., Stein, A., Van Der Meer, F., Gorte, B. (1999). Accuracy assessment of spatial information, in Spatial Statistics for Remote Sensing, Remote Sensing and Digital Image Processing. *Springer Netherlands, Dordrecht,* 197–209. doi: 10.1007/0-306-47647-9_12

Tejasree, G., Agilandeeswari, L., (2024). Land use/land cover (LULC) classification using deep-LSTM for hyperspectral images. Egypt. J. Remote Sens. *Space Sci.* 27, 52–68. https://doi.org/10.1016/j.ejrs.2024.01.004

Teshager, Z., & Abeje, K. (2021). GIS and Remote Sensing based Land Us e/Land Cover Change Detection: The Case of Kility Watershed. *J Remote Sens GIS,* 10(3). doi: 10.35248/2469-4134.21.10.282

UN. (2019). *Sustainable Development Goals Report.* Retrieved from https://unstats.un.org/sdgs/report/2019/

Vajsova, B., & Aastrand, P. (2015). *New sensors benchmark report on Sentinel-2A.* Retrieved from https://ec.europa.eu/jrc

Vaughn, I. (2019). *Landsat 8 (L8) Data Users. Handbook.* Retrieved From https://www.usgs.gov/media/files/landsat-8-data-users-handbook

Wulansari, H. (2017). Uji Akurasi Klasifikasi Penggunaan Lahan Dengan Menggunakan Metode Defuzzifikasi Maximum Likelihood Berbasis Citra Alos Avnir-2. BHUMI J. *Agrar. Dan Pertanah.,* 3, 98. doi: 10.31292/jb.v3i1.233

Xu, P., Tsendbazar, N.-E., Herold, M., De Bruin, S., Koopmans, M., Birch, T., Carter, S., Fritz, S., Lesiv, M., Mazur, E., Pickens, A., Potapov, P., Stolle, F., Tyukavina, A., Van De Kerchove, R., Zanaga, D., 2024. Comparative validation of recent 10 m-resolution global land cover maps. Remote Sens. *Environ,* 311, 114316. doi: 10.1016/j.rse.2024.114316

Zaabar, N., Niculescu, S., Mihoubi, M.K. (2023). Assessment of Land Cover Changes in the Allala Watershed Based on Object Based Image Analysis Using Landsat and Sentinel-2 Images, in:in : Niculescu, S. (Ed.), European Spatial Data for Coastal and Marine Remote Sensing. *Springer International Publishing*, Cham, 81–96. doi: 10.1007/978-3-031-16213-8_5

Zafar, Z., Zubair, M., Zha, Y., Fahd, S., Ahmad Nadeem, A., (2024). Performance assessment of machine learning algorithms for mapping of land use/land cover using remote sensing data. Egypt. *J. Remote Sens. Space Sci.* 27, 216–226. doi: 10.1016/j.ejrs.2024.03.003